Electronic Supplementary Material (ESI) for Journal of Materials Chemistry A.

Supplementary Information

Improving Selectivity of CO Reduction *via* Reducing Coordination of Critical Intermediate

Yifan Li [a,b], † Yumin Qian [a], † Yujin Ji [a], Hui Li [b,*], Yuanyue Liu [a,*]

[a] Texas Materials Institute and Department of Mechanical Engineering

The University of Texas at Austin, Austin, TX, 78712

[b] Key Laboratory for Liquid−Solid Structural Evolution and Processing of Materials, Ministry of Education, Shandong University, Jinan 250061, People's Republic of China

* Corresponding author:

lihuilmy@hotmail.com

Yuanyue.liu@austin.utexas.edu

Rationalization of the definition of the CO adsorption energy

We used this definition (1) because our calculations show that it is energetically favorable to adsorb two CO molecules, i.e. the energy change for the second CO adsorption is downhill, regardless of which metal site the first CO is adsorbed on; (2) In reality, a relatively high concentration of CO is transported to the catalyst surface during reaction. Therefore, 2CO adsorption is likely from both thermodynamic and kinetic points of view, which rationalize our definition of adsorption energy.

Discussion about the monotonic correlation between CO adsorption energy and CO-CO coupling energy

As shown in Figure 2 (b), a weaker CO adsorption leads to a stronger CO-CO coupling. The V-Mo has the weakest binding with CO and thus results in the strongest CO-CO coupling.

To understand this phenomenon, we hypothesize that when the CO is adsorbed on a metal atom, the lone pair electrons of C will interact with the metal d orbital (see Figure S3), which chemically activates the C. Thus the C atoms in neighboring adsorbed CO molecules can couple with each other through their p orbitals. On the other hand, the metal atom can transfer charge to the C atom, which may partially saturate its p orbitals for coupling. Indeed, we find that when CO is adsorbed, the C atom gets electron from the metal atom (see Table S2 and Figure S4); and the coupling strength decreases with more electron transferred (see Figure S5), supporting our hypothesis. Since the charge transfer is also correlated with the adsorption energy (weaker adsorption leads to a larger separation between C and metal (Table S3) and thus a less charge transfer (Figure S5)), the coupling energy appears to be negatively correlated with the adsorption energy in these cases.

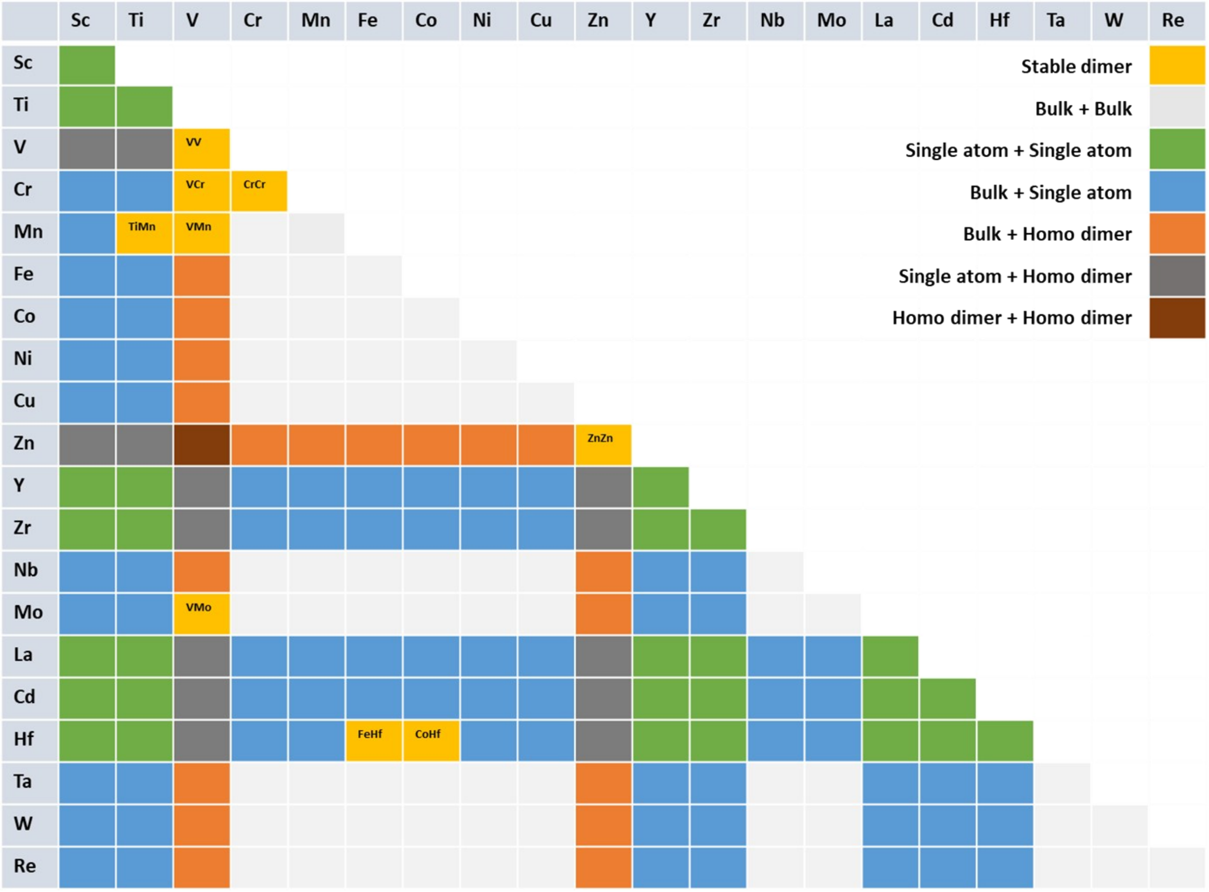

	Sc	Ti	V	Cr	Mn	Fe	Co	Ni	Cu	Zn	Y	Zr	Nb	Mo	La	Cd	Hf	Ta	W	Re
Sc	🟩																			
Ti	🟩	🟩																		
V	⬛	⬛	🟨 VV																	
Cr	🟦	🟦	🟨 VCr	🟨 CrCr																
Mn	🟦	🟨 TiMn	🟨 VMn	⬜	⬜															
Fe	🟦	🟦	🟧	⬜	⬜	⬜														
Co	🟦	🟦	🟧	⬜	⬜	⬜	⬜													
Ni	🟦	🟦	🟧	⬜	⬜	⬜	⬜	⬜												
Cu	🟦	🟦	🟧	⬜	⬜	⬜	⬜	⬜	⬜											
Zn	⬛	⬛	🟫	🟧	🟧	🟧	🟧	🟧	🟧	🟨 ZnZn										
Y	🟩	🟩	⬛	🟦	🟦	🟦	🟦	🟦	🟦	⬛	🟩									
Zr	🟩	🟩	⬛	🟦	🟦	🟦	🟦	🟦	🟦	⬛	🟩	🟩								
Nb	🟦	🟦	🟧	⬜	⬜	⬜	⬜	⬜	⬜	🟧	🟦	🟦	⬜							
Mo	🟦	🟦	🟨 VMo	⬜	⬜	⬜	⬜	⬜	⬜	🟧	🟦	🟦	⬜	⬜						
La	🟩	🟩	⬛	🟦	🟦	🟦	🟦	🟦	🟦	⬛	🟩	🟩	🟦	🟦	🟩					
Cd	🟩	🟩	⬛	🟦	🟦	🟦	🟦	🟦	🟦	⬛	🟩	🟩	🟦	🟦	🟩	🟩				
Hf	🟩	🟩	⬛	🟦	🟦	🟨 FeHf	🟨 CoHf	🟦	🟦	⬛	🟩	🟩	🟦	🟦	🟩	🟩	🟩			
Ta	🟦	🟦	🟧	⬜	⬜	⬜	⬜	⬜	⬜	🟧	🟦	🟦	⬜	⬜	🟦	🟦	🟦	⬜		
W	🟦	🟦	🟧	⬜	⬜	⬜	⬜	⬜	⬜	🟧	🟦	🟦	⬜	⬜	🟦	🟦	🟦	⬜	⬜	
Re	🟦	🟦	🟧	⬜	⬜	⬜	⬜	⬜	⬜	🟧	🟦	🟦	⬜	⬜	🟦	🟦	🟦	⬜	⬜	⬜

Stable dimer	🟨
Bulk + Bulk	⬜
Single atom + Single atom	🟩
Bulk + Single atom	🟦
Bulk + Homo dimer	🟧
Single atom + Homo dimer	⬛
Homo dimer + Homo dimer	🟫

Figure S1: All transition metal element screened, and the low energy structures for each atom element and their combinations. Different colors are used to represent different combinations.

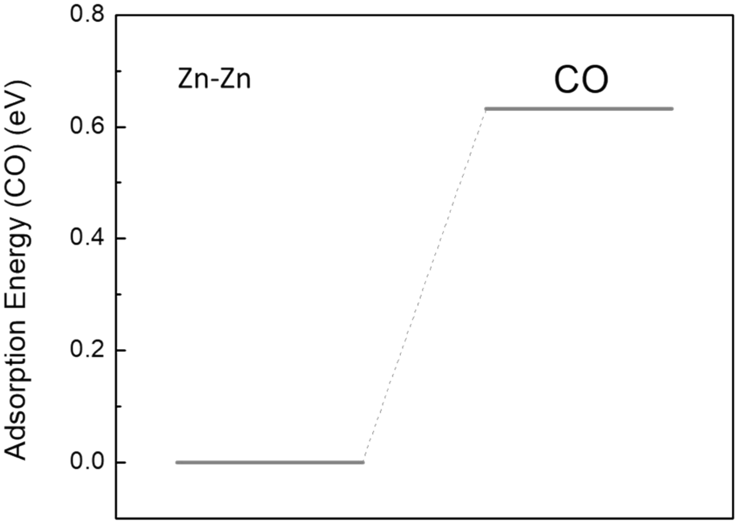

Figure S2: Adsorption free energy of one CO on Zn-Zn

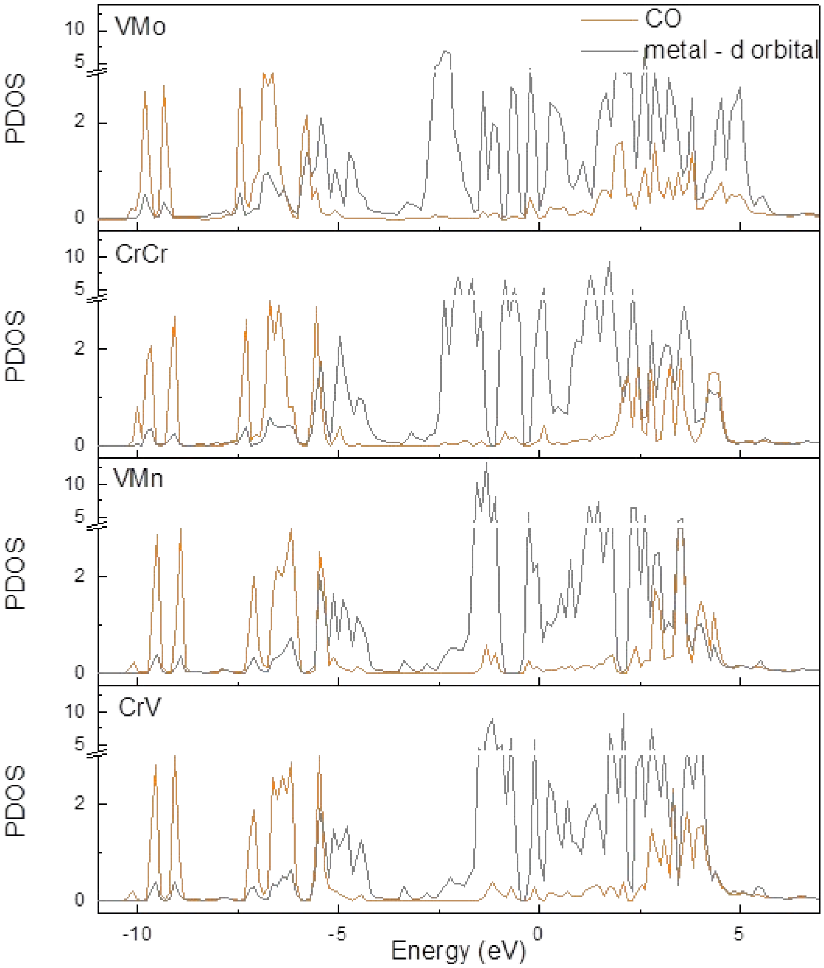

Figure S3: Projected density of state (PDOS) plot of the d orbital of transition metal atoms and the C atoms in adsorbed CO in four metal-C_2N systems.

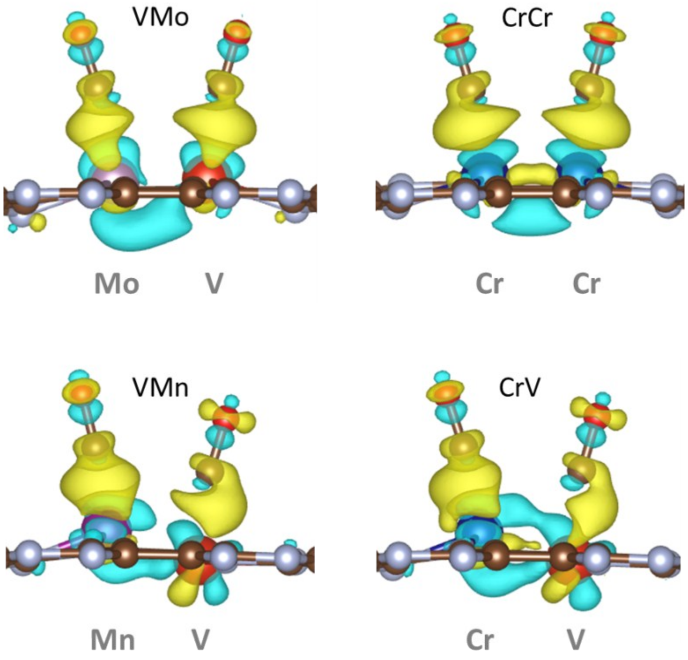

Figure S4: Electron density change due to CO adsorption. Yellow represents electron density accumulation while green means depletion.

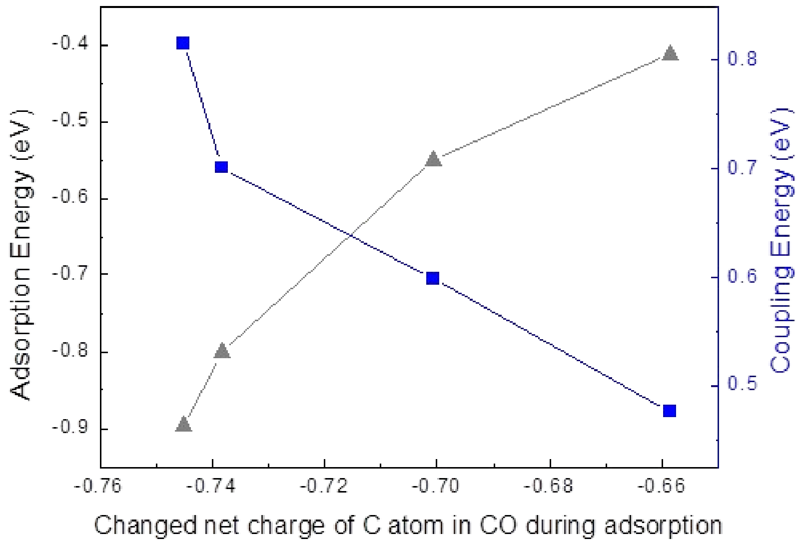

Figure S5: Adsorption energy and CO-CO coupling energy as a function of the charge variation in C atoms during two CO adsorption.

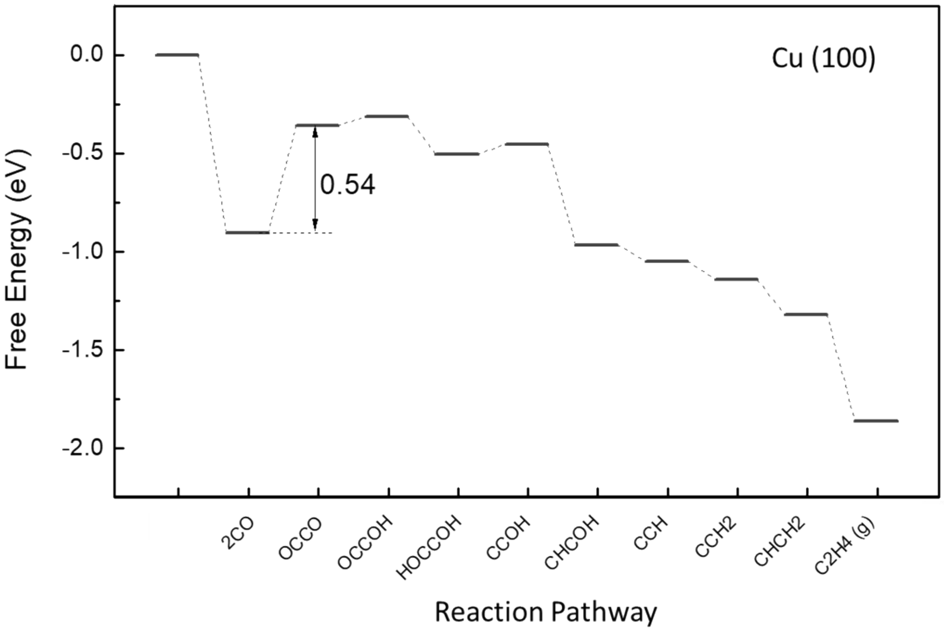

Figure S6: Free energy profile for the CO reduction to C_2H_4 on Cu (100) surface at 0 V vs RHE.

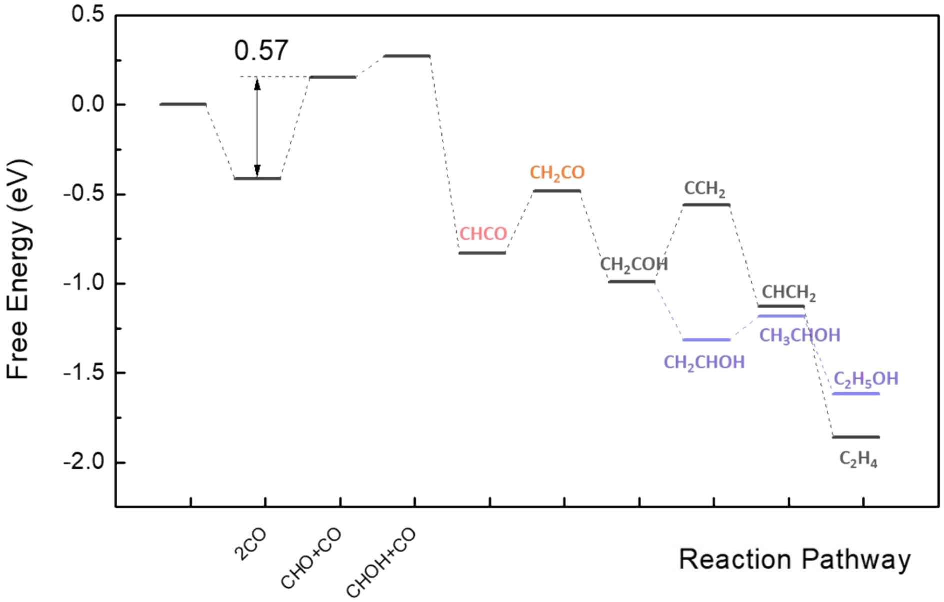

Figure S7: Free energy profile for the CO reduction along the CH4 formation pathway on V-Mo at 0 V vs RHE

Table S1: The relative energies of nine stable dimers and their other possible configurations. The formation energies of dimers are scaled to zero and the energies of other possible combinations are relative value. these dimers are considered to be stable because they have the lowest formation energies or close to the lowest formation energies (<0.2 eV) comparing with other possible configurations.

B: Bulk S: single atoms anchored on C_2N D: homonuclear dimer anchored on C_2N; A, B: two transition metal

	hetero-dimer	B_A+B_B	B_A+S_B	B_A+D_B	S_A+B_B	S_A+S_B	S_A+D_B	D_A+B_B	D_A+S_B	D_A+D_B
CrV	0	0.075	0.618	-0.081	0.834	1.376	0.677	0.159	0.701	0.003
FeHf	0	0.331	-0.071	0.988	1.312	0.910	1.969	0.880	0.478	1.537
VMn	0	0.146	0.688	-0.010	0.183	0.725	0.027	0.406	0.948	0.249
TiMn	0	0.275	-0.022	0.288	0.311	0.015	0.324	0.534	0.238	0.547
VMo	0	0.188	0.730	0.031	1.595	2.137	1.438	0.597	1.140	0.441
CoHf	0	0.324	-0.078	0.981	1.215	0.813	1.872	0.989	0.587	1.646
	homo-dimer	Bulk				Single atom				
CrCr	0	-0.168	-	-	-	1.349		-	-	-
VV	0	0.313	-	-	-	1.398		-	-	-
ZnZn	0	0.140	-	-	-	0.499		-	-	-

Table S2: The distance between adsorbed CO and two metal atoms. Only the CO closer to the metal atoms is shown.

	C-metal A (Å)	C-metal B (Å)	Total distance (Å)
VMo	1.97868	2.99167	4.97035
CrCr	2.87747	1.86473	4.7422
VMn	2.54056	1.90253	4.44309
CrV	1.91338	2.53444	4.44782